Solid Freeform Fabrication 2023: Proceedings of the 34th Annual International Solid Freeform Fabrication Symposium – An Additive Manufacturing Conference
Reviewed Paper

LIQUID METAL JETTING OF ALUMINUM PARTS WITH SALT SUPPORT STRUCTURES

Benedikt Kirchebner[1,*], Christoph Weidner[1], Maximilian Ploetz[1], Christoph Rehekampff[2], Wolfram Volk[1], Philipp Lechner[1]

[1]Technical University of Munich, Germany; TUM School of Engineering and Design, Department of Mechanical Engineering, Chair of Metal Forming and Casting

[2]Technical University of Munich, Germany; TUM School of Engineering and Design, Department of Mechanical Engineering, Institute of Micro Technology and Medical Device Technology

*Corresponding author: benedikt.kirchebner@tum.de

Abstract

Liquid metal jetting (LMJ) bears the potential of being a fast part manufacturing technology while using a cheap raw material. LMJ is a subtype of material jetting (MJT) and the parts are built by successively depositing droplets of molten metal onto a build platform. For full 3D capability, support structures are necessary, which must be removed in subsequent processes. In previous investigations, we proposed the usage of water-soluble salt as a support material, selected a suitable salt, and analyzed the influence of this material on aluminum parts made in LMJ. The present work shows a duplex MJT print head for processing aluminum alloys and KCl-NaCl salt. Various printing sequences and support structure strategies are compared. The results show that the sequence of printing aluminum and salt is crucial. Furthermore, using thin layers of the support material as a release layer appears promising.

Keywords: Liquid metal jetting, Liquid salt jetting, Support structures, Additive manufacturing

1. Introduction

Liquid metal jetting (LMJ) is an additive manufacturing (AM) technology that can be used to manufacture near-net-shape metal parts. Molten metal, e.g., aluminum or copper, is ejected through a nozzle as droplets. This can be done either by a continuous droplet stream (continuous jet) [1] or droplet by droplet (drop on demand) [2]. For the ejection of the droplets, various principles are used, e.g., pneumatic [3], piezoelectric [4], or magnetohydrodynamic [5]. The resolution of the printed parts is determined by the diameter of the metal droplets. The droplet diameter itself heavily depends on the setup and is typically in the range of 50 µm to 1.3 mm [6]. Since the printing frequency of all ejection systems is limited, the droplet diameter not only influences the printing resolution but also limits the amount of jetted material per time. Therefore, small droplets are not always desirable, especially when considering the cubic relationship between the diameter and the volume of a sphere. In the literature, the LMJ of aluminum [7], silver [8], copper [9], steel [10], and other materials have been reported. A broad overview of the state of the art of liquid metal jetting was published by Ansell et al. [6].

One of the main advantages of LMJ is the ability to use a wire as a raw material, which is typically cheaper and easier to handle than metal powder [11]. Further, LMJ does not require downstream sinter processes, is highly scalable, and allows the fabrication of multi-material parts [12]. The voxel-based approach of LMJ opens up the field of local material optimization. Varying thermal process conditions in LMJ significantly influence the mechanical properties of jetted aluminum parts. The mechanical properties of jetted parts can outperform cast parts if the thermal conditions in LMJ are optimal [13].

A big advantage of AM is the design freedom; however, all AM processes have limitations in the capability of realizing three-dimensional (3D) structures. A challenge in LMJ is the fabrication of complex geometries with overhanging structures since the incline angle is limited [14]. To some extent, this issue can be approached by using an LMJ system with more than three spatial degrees of freedom, e.g., one with a tilting or rotating build platform [15]. In more general cases, full 3D capability can be attained by using support structures. One approach is to print the support structures from the same material as the final part (build material). However, the support structures must be removed after the manufacturing process in many cases, which can be challenging. Support removal via machining adds a post-processing step to the manufacturing chain, and the support structures must be accessible in the first place, which in turn can reduce design freedom. This also holds for manual support removal, which can be reasonable in small batches. In any case, the quality of the final part must be considered, especially in the areas where the support connects to the final part. Further, there is always the risk of damaging the final part [16]. Additionally, just like the final part, the support structures must be manufactured, which takes pre-processing time, raw material, and processing time, thus increasing cost [17]. An approach to solving many of these issues is using support structures that can be removed by dissolution. Soluble support structures have already been applied in other AM processes, such as fused deposition modeling with water-soluble poly(vinyl alcohol) support [18], direct energy deposition with carbon steel support that is removed by electrochemical etching with nitric acid [19], and powder bed fusion with a similar approach to the latter [20]. For LMJ, we investigate the use of salts for water-soluble support structures. The expected advantages of this approach are an easy support removal with no damage to the final part and little influence on the printing process. In analogy to LMJ, the salt support structures shall be processed by jetting, too. We call this process liquid salt jetting (LSJ). Figure 1 depicts a schematic of a part jetted from a build material (shown in blue) with a support structure made from a soluble support material (shown in green) via LSJ. The part geometry is inspired by the logo of the Technical University of Munich (TUM). The part is jetted onto a printing plate (shown in black), which sits on a heated build platform, as described in the Materials and Methods section.

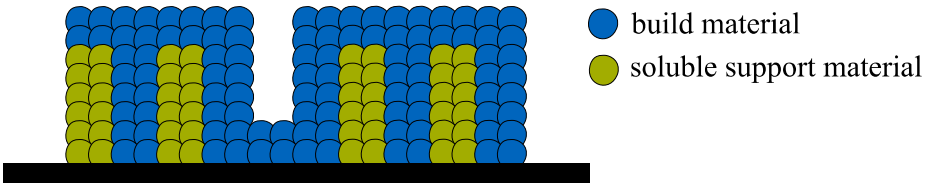

Figure 1: Schematic of a part manufactured in the liquid metal jetting (LMJ) process with a soluble support structure made via liquid salt jetting (LSJ). The part geometry is inspired by the logo of the Technical University of Munich (TUM).

Salt melts are often highly wetting [12] and corrosive [21, 22], thus making the material selection for the print head a challenging task. Suitable salts were selected in previous investigations, and a material jetting print head was developed, built, and tested. Demonstrator parts could be produced via LSJ [12]. In a subsequent study, the influence of jetting molten salt on jetted aluminum parts was analyzed. No significant signs of corrosion of the jetted aluminum parts by the molten salt were observed. However, the microstructure of the aluminum just on top of the support was coarser than in other areas with the same vertical distance to the printing plate [23]. A possible explanation for this phenomenon is the reduced heat conduction due to the lower thermal conductivity of the used salts – KCl and NaCl [24] – compared to aluminum [25]. Heat conduction is, among other factors, an essential task of support structures in metal AM [17].

Summing up the existing research, the processing of molten salt in a jetting process is possible and its use as a support structure for LMJ has been demonstrated. A still open field is the probing of the limits of LSJ and the comparison of different support structure strategies. Both of these topics are addressed in this paper.

2. Materials and Methods

2.1. Build and Support Material

As build material for all jetted parts in this work, an aluminum alloy with 12 % silicon (AlSi12, also denoted by 4047 or LM6) is used. AlSi12 has a liquidus temperature of 590 °C, taking the average value for the liquidus temperature in the cooling and the heating cycle into account [26]. The raw material is a rod with 2 mm in diameter and 1 m in length (VDB-Schweisstechnik, Dormagen, Germany). As soluble material for the support structures, a eutectic mixture of potassium chloride (KCl) and sodium chloride (NaCl) is used. According to Bale et al., the NaCl content in the eutectic mixture is 50.6 mol % and the liquidus temperature is 657 °C [27]. This mixture, which is denoted by KCl-NaCl, was selected in previous investigations to be processed via jetting in the molten state [12]. KCl and NaCl are sourced separately, with a purity of ≥ 99,5 % for KCl and ≥ 99,8 % for NaCl (Carl Roth GmbH + Co. KG, Karlsruhe, Germany). The raw materials are in powder form and mixed in the crucible before processing.

2.2. Experimental Setup

All experiments were performed on a self-constructed MJT test stand. The test stand is a further development of the system previously described by Himmel et al. [13] and can be equipped with various print heads. The print heads sit on top of a nitrogen-purged process chamber. Inside this chamber is a heated build platform that can move in three spatial directions, driven by an axis system below the chamber. A pneumatic duplex print head for processing AlSi12 and KCl-NaCl is used in the present work. The LSJ system is based on a design that was described in previous work [12]. The print head ejects droplets pneumatically via a pressure surge that is controlled by a pressure regulator and a solenoid valve. The duplex print head consists of two heated crucibles, each with a nozzle plate on the bottom. The raw material (AlSi12 rod or KCl-NaCl powder) is melted inside the crucible and jetted through the nozzle by pneumatic pressure surges. The oxygen

content in the process chamber is close-loop controlled. A schematic of the MJT test with the duplex print head is depicted in Figure 2 and a picture of the test stand is shown in Figure 3.

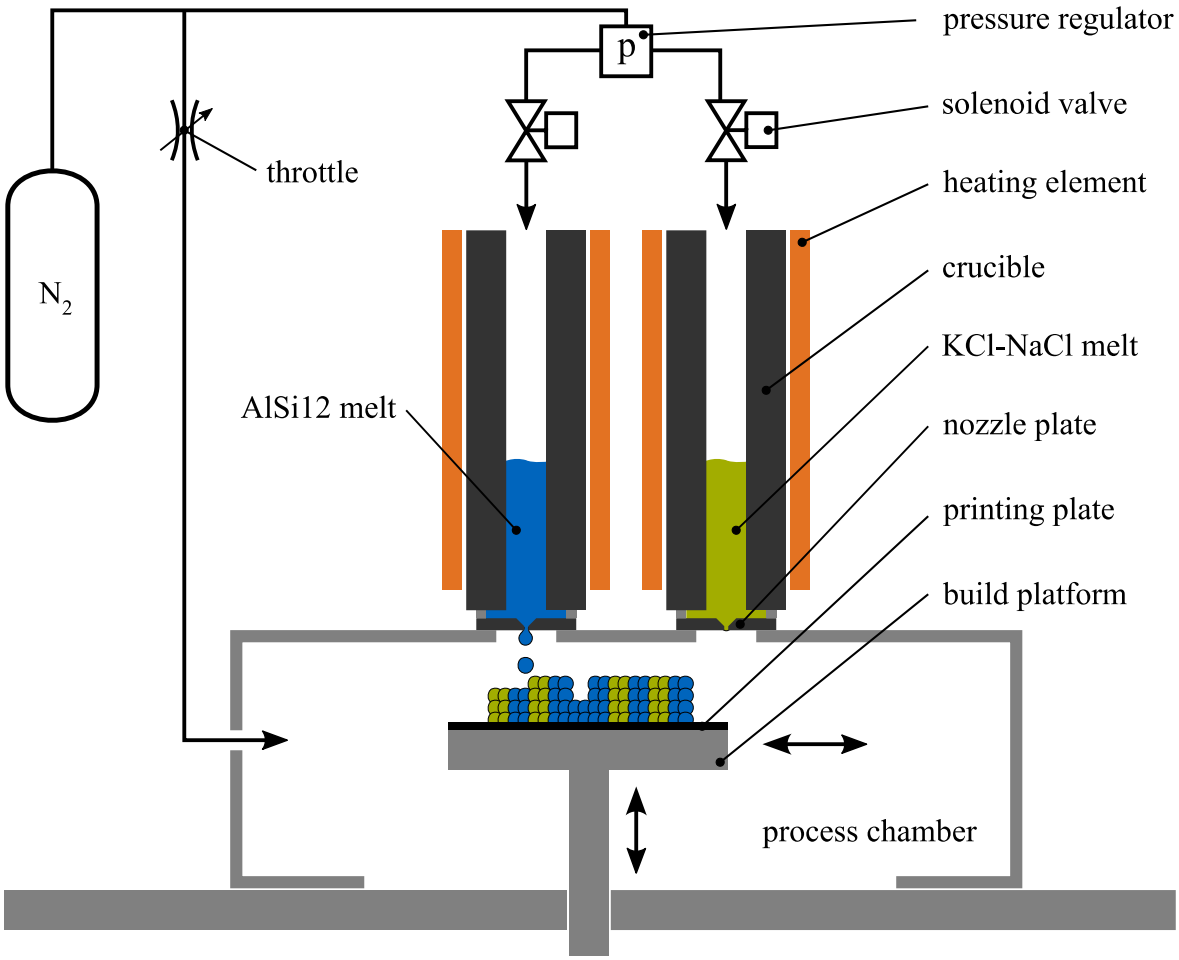

Figure 2: Schematic of the MJT test stand with the duplex print head for LMJ and LSJ. The print head consists of two heated crucibles, each with a nozzle plate on the bottom. Droplets are ejected onto a printing plate that is placed on top of a heated, movable build platform. The pneumatic droplet ejection is realized by a pressure regulator and solenoid valves. The process chamber is nitrogen-purged.

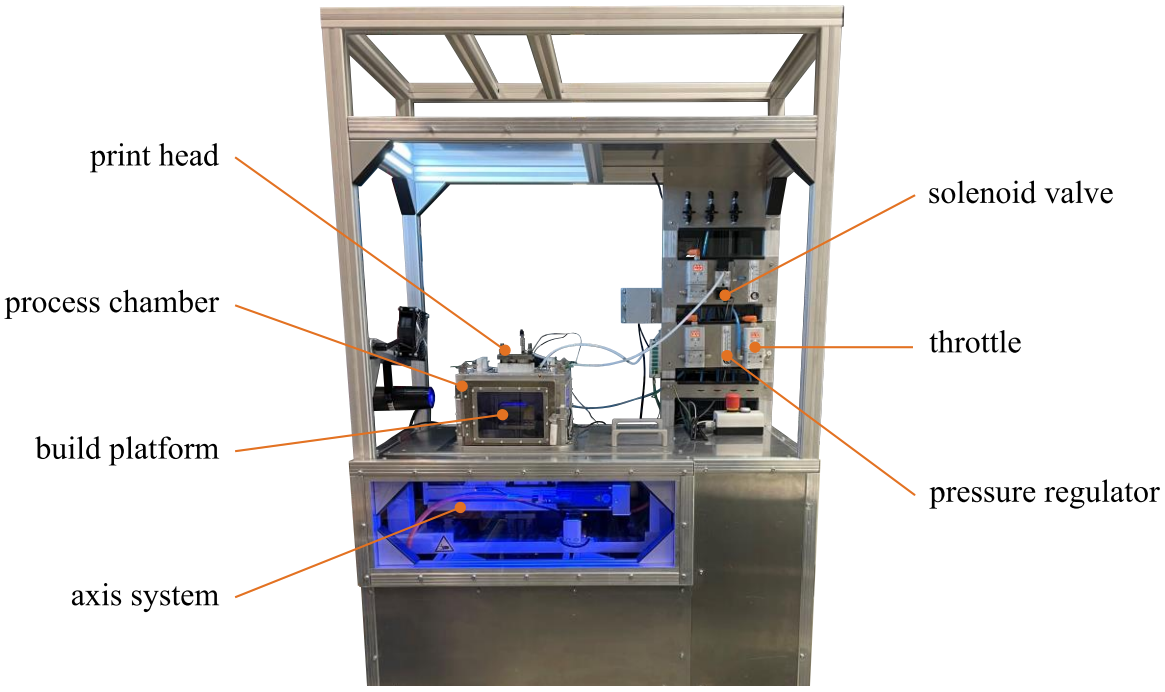

Figure 3: Picture of the MJT test stand. In the center of the stand is the process chamber with the heated build platform inside. The print head is located on top of the process chamber, next to the pneumatic system with pressure regulators, throttles and solenoid valves. Below the process chamber is the axis system that drives the heated build platform. The picture only shows the upper part of the MJT test stand. The total height of the MJT test stand is 2m.

2.3. Experimental Procedure

To investigate the two main areas of this work – probing the limits of LSJ and investigating different support structure strategies – test specimens are fabricated on the MJT test stand and the results are evaluated qualitatively. To examine the limitations of LSJ, first, pillars are printed at different angles to determine the realizable overhangs. These inclined pillars can be used to create geometrically optimized branched support structures. Secondly, the relevance of the printing sequence is investigated. It is known from previous experiments that the adhesion of AlSi12 to KCl-NaCl is limited and mainly based on form-fit. By means of a test geometry with several layers of AlSi12 and KCl-NaCl, the influence of different printing sequences on the printing result shall be investigated. To compare different support structure concepts, a sample geometry (TUM logo) is printed three times, each time with a different type of support structure strategy. The printed TUM logos are then examined qualitatively. The test geometries are described in detail in the following chapters. A flow chart of the complete experimental procedure of this work is shown in Figure 4. For the fabrication of all samples of this investigation, the process parameters listed in Table 1 are used.

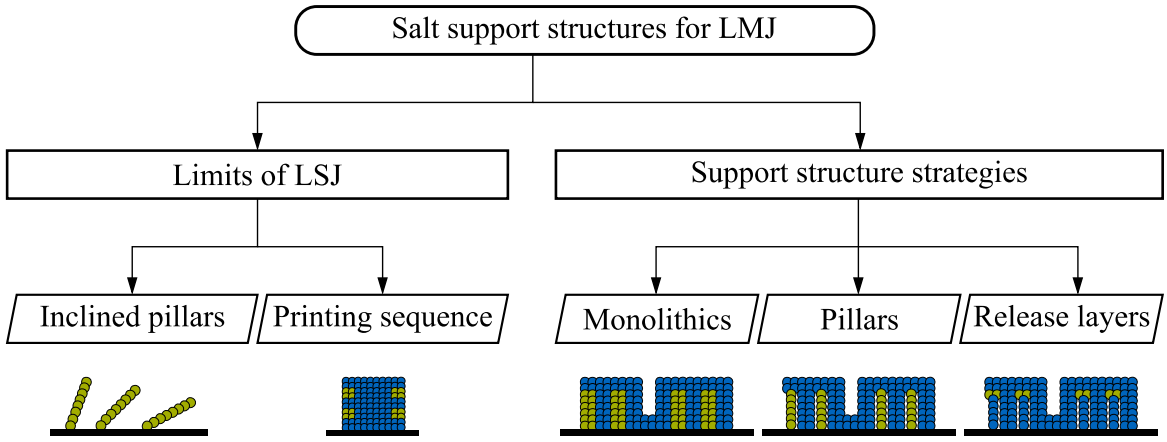

Figure 4: Flow chart of the experimental procedure for examining salt support structures for liquid metal jetting (LMJ). First, the limits of liquid salt jetting (LSJ) are investigated and then, different support structure strategies are compared.

Table 1: Parameters for processing AlSi12 and KCl-NaCl on the MJT test stand.

Parameter	**Value**
Build platform temperature	500 °C
Oxygen content in chamber	< 100 ppm
Processing temperature AlSi12	700 °C
Mean droplet diameter AlSi12	1,1 mm
Printing frequency AlSi12	5 Hz
Pneumatic pressure AlSi12	1,5 bar
Valve opening time AlSi12	2 ms
Processing temperature KCl-NaCl	800 °C
Mean droplet diameter KCl-NaCl	0,7 mm
Printing frequency KCl-NaCl	1,5 Hz
Pneumatic pressure KCl-NaCl	3,5 bar
Valve opening time KCl-NaCl	4 ms

2.3.1. Limits of LSJ

Salt pillars with different inclination angles shall demonstrate the geometric limits of LSJ. The pillars are fabricated by ejecting droplets on a moving printing plate at varying droplet spacings to form different inclination angles. The droplet spacings are 50 µm, 125 µm, and 150 µm.

A more complex part, produced by combining LSJ and LMJ, is used to demonstrate the importance of the sequence of printing build and support material. The geometry is inspired by a cylindrical heat sink and requires the fabrication of multiple layers of AlSi12 and KCl. The part is referred to as *demo part* and is depicted in Figure 5 from the front (a), in section view (b), and in section view support structure (c).

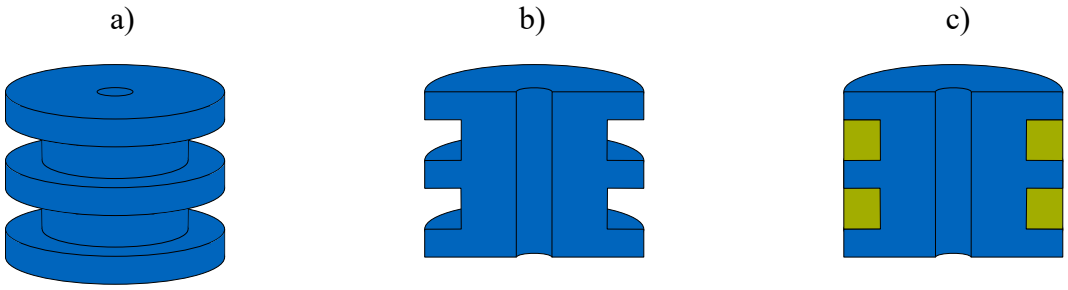

Figure 5: Demo part to compare different printing sequences. Depicted from the front (a), in section view (b), and in section view with support structure (c).

The layers of the part can be fabricated according to several ways. Two of them are investigated in this paper. Figure 6 shows a top view of the sample with an AlSi12 and a KCl-NaCl layer already printed and the first few AlSi12 droplets of the next layer. In subfigure (a), these AlSi12 droplets are ejected circularly, starting from the center of the part, so that the AlSi12 droplets come into contact with AlSi12 droplets from the previous layer. In subfigure (b), the AlSi12 droplets for the next layer are also ejected in a circular fashion, but starting from the outside and initially only touching the KCl-NaCl droplets of the previous layer.

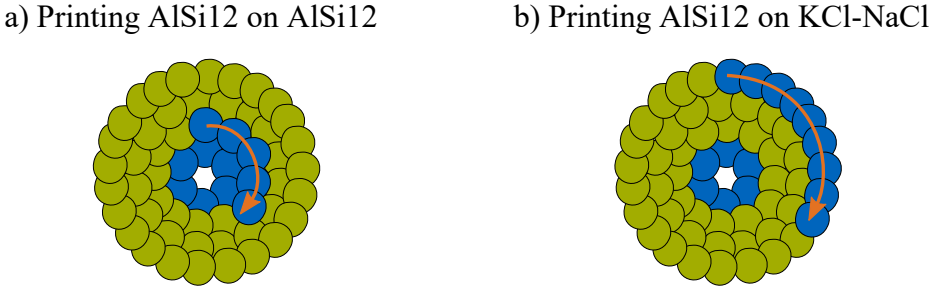

Figure 6: Printing sequences for the demo part. Starting to print the AlSi12 layer from the center of the part, with AlSi12 contacting AlSi12 (a) and starting to print the AlSi12 layer from the outside of the part, with AlSi12 initially contacting KCl-NaCl only (b).

2.3.2. Support structure strategies

As previously described, three different strategies to realize salt support structures for LMJ of aluminum are realized and discussed in this work. The trivial strategy for salt support structures in LMJ is fabricating monolithic salt blocks. As a first optimization approach, we will discuss pillar support structures to reduce build-up time and material use. The third strategy is the use of salt only as a releasing layer between an aluminum support structure and the aluminum part. The idea behind these so-called release layer support structures is an improvement of the heat transfer through the support, which influences part quality, as shown in previous work [23]. As for comparing the support structure strategies, TUM logos are fabricated on the MJT test stand. A schematic of all support structure strategies is shown in Figure 7.

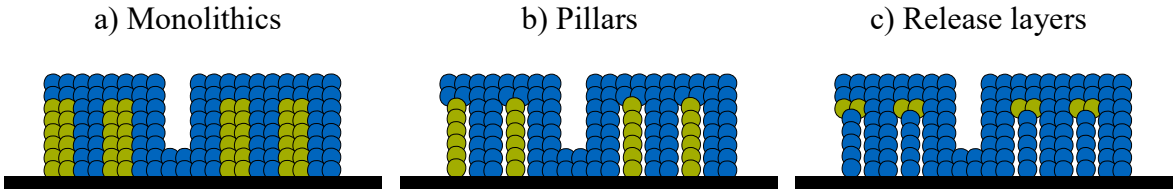

Figure 7: Strategies for producing soluble salt support structures: (a) monolithic salt support structure, (b) salt pillar support structure, (c) salt release layer support structure.

3. Results and Discussion

3.1. Limits of LSJ

The printed salt pillars are shown in Figure 8. For droplet spacings of 50 µm and 125 µm, straight pillars form at angles of approximately 70° and 45°, respectively. In the case of 125 µm droplet spacing, the pillar is warped slightly. Wider droplet spacings, and thus shallower angles, are more challenging. At a droplet spacing of 150 µm, the pillars collapse repeatedly. It appears that the practical limit for overhangs in LSJ is an inclination angle of 45° – similar to the maximum inclination angle in LMJ of aluminum [14].

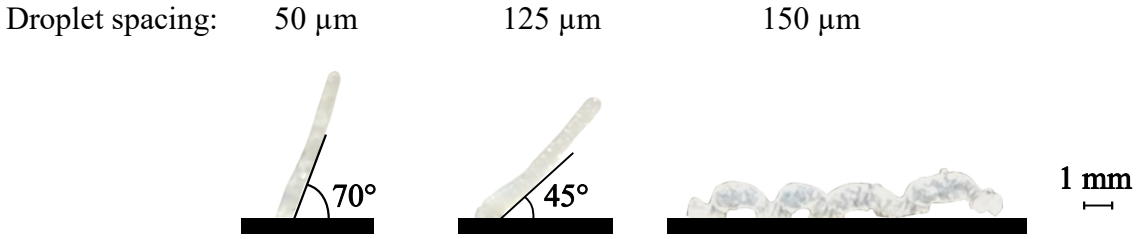

Figure 8: Salt pillars printed at different droplet spacings (50 µm, 125 µm, and 150 µm).

Two demo parts for comparing different printing sequences are depicted in Figure 9. For each printing sequence, a schematic representation and the printed part is shown. The initial adhesion of AlSi12 droplets to KCl-NaCl in the fabrication process is limited and mainly based on form-fit. In many cases, AlSi12 droplets bounce off the KCl-NaCl layer, causing geometric deviations. Further, due to the low heat conduction of KCl-NaCl, neighboring AlSi12 droplets join to form larger droplets, which in turn leads to deviations from the desired geometry. Both defects are visible in subfigure (b). Therefore, AlSi12 droplets should initially always land on AlSi12, as is the case in subfigure (a). A demo part that was fabricated according to this sequence (AlSi12 on AlSi12) is shown in Figure 10 as a schematic (a), as a printed part with support (b), and as a printed part without support (c).

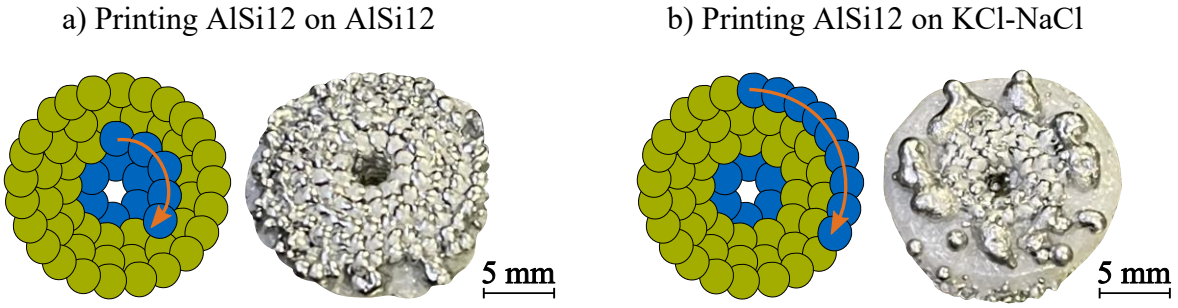

Figure 9: Comparison of printing sequences. Starting to print the AlSi12 layer from the center of the part with AlSi12 droplets contacting AlSi12 (a) and starting to print the AlSi12 layer from the outside with AlSi12 droplets contacting KCl-NaCl only (b).

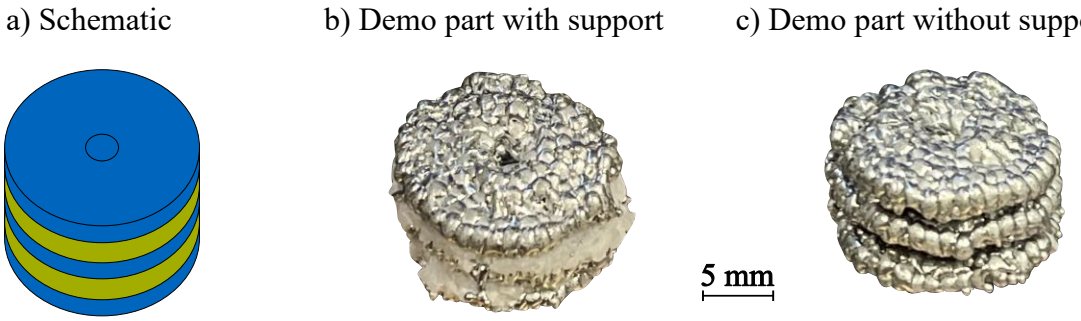

Figure 10: Demo part, fabricated according to the AlSi12 on AlSi12 sequence. Schematic (a), printed part with support structure (b), and printed part after support structure removal (c).

3.2. Support structure strategies

The TUM logo fabricated with monolithic salt support structure is shown in Figure 11. A schematic of the part is shown in (a), the part with support is shown in (b), and the part after support removal is shown in (c). The geometrical deviations are due to a variation in the individual droplet size of AlSi12 and KCl-NaCl. This is caused by irregularities in the pressure surge, among other things. The total printing time for the part with support is 10 min and 30 s.

Figure 11: TUM logo with monolithic salt support structure. Schematic (a), printed part with support structure (b), and printed part after support structure removal (c).

The TUM logo fabricated with a salt pillar support structure is shown in Figure 12. A schematic of the part is shown in (a), the part with support is shown in (b), and the part after support removal is shown in (c). Compared with the monolithic support structure, only about one third of

the KCl-NaCl droplets are printed, resulting in a time saving of 2 min 25 s at a total printing time of 8 min 5s. The geometric fidelity of the part with pillar support and the part with monolithic support is similar.

Figure 12: TUM logo with salt pillar support structure. Schematic (a), printed part with support structure (b), and printed part after support structure removal (c).

The TUM logo with salt release layer support structures is shown in Figure 13. A schematic of the part is shown in (a), the part with support is shown in (b), and the part after support removal is shown in (c). The total printing time for the part is 6 min 40 s which is 1 min 25 s faster than the printing time of the TUM logo with pillar support structure. The release layer support structure is hardly visible since it is only two droplet layers thick, and some AlSi12 droplets overlap the release layer laterally. The support structure columns are partially bonded to the part, making support structure removal difficult. The geometric fidelity of the part is inferior to the parts with monolithic and pillar supports. A proposed solution for this issue is an adjustment of the spacing of pillars and part, if applicable, with the use of fanned-out tree supports.

Figure 13: TUM logo with salt release layer support structure. Schematic (a), printed part with support structure (b), and printed part after support structure removal (c).

4. Summary and Outlook

The objective of this paper was to investigate soluble support structures for aluminum LMJ that are fabricated via liquid salt jetting (LSJ). First, the limitations of LSJ were analyzed using two test geometries. The results show that KCl-NaCl pillars can be printed with an overhang angle of up to 45°. Attention must be paid to the printing sequence since the initial adhesion of AlSi12 droplets to KCl-NaCl is limited. It is advisable to let the AlSi12 droplets of a new layer come into contact with the AlSi12 droplets of the previous layer. This paper's second object of investigation was the comparison of different support structure strategies. Parts with monolithic support structure, pillar support structure, and release layer support structure were fabricated. A comparable geometric fidelity was obtained with monolithic and pillar support structures; however, salt pillar support structures offer the advantage of a shorter printing time and less material consumption. Release layer support structures offer the potential of the least thermal influence on the process, which, referring to previous studies [23], has a positive effect on the mechanical strength of AlSi12 components. This work provides a qualitative examination of salt

support structures for LMJ. Further investigations and quantitative characterizations of printed test specimens are needed for more detailed statements.

The thermal impact of support structures in LMJ could be further optimized by using release layer support structures with thinner release layers and by using a release material with better thermal conductivity. In future work, thinly sprayed-on graphite as a release layer shall be examined.

Acknowledgments

The authors thank the German Research Foundation for funding this research (project number: 420547518).

References

1. Liu Q, Orme M (2001) On precision droplet-based net-form manufacturing technology. Proceedings of the Institution of Mechanical Engineers, Part B: Journal of Engineering Manufacture 215:1333–1355. https://doi.org/10.1243/0954405011519123
2. Cheng S, Chandra S (2003) A pneumatic droplet-on-demand generator. Exp Fluids 34:755–762. https://doi.org/10.1007/s00348-003-0629-6
3. Tropmann A, Lass N, Paust N et al. (2012) Pneumatic dispensing of nano- to picoliter droplets of liquid metal with the StarJet method for rapid prototyping of metal microstructures. Microfluid Nanofluid 12:75–84. https://doi.org/10.1007/s10404-011-0850-1
4. Orme M, Smith RF (2000) Enhanced Aluminum Properties by Means of Precise Droplet Deposition. Journal of Manufacturing Science and Engineering 122:484–493. https://doi.org/10.1115/1.1285914
5. Sukhotskiy V, Karampelas IH, Garg G et al. (2017) Magnetohydrodynamic Drop-on-Demand Liquid Metal 3D Printing. Proceedings of the 28th Annual International Solid Freeform Fabrication Symposium 1:1806–1811. https://doi.org/10.26153/tsw/16905
6. Ansell TY (2021) Current Status of Liquid Metal Printing. JMMP 5:31. https://doi.org/10.3390/jmmp5020031
7. Chao Y, Qi L, Xiao Y et al. (2012) Manufacturing of micro thin-walled metal parts by micro-droplet deposition. Journal of Materials Processing Technology 212:484–491. https://doi.org/10.1016/j.jmatprotec.2011.10.015
8. Simonelli M, Aboulkhair N, Rasa M et al. (2019) Towards digital metal additive manufacturing via high-temperature drop-on-demand jetting. Additive Manufacturing 30:100930. https://doi.org/10.1016/j.addma.2019.100930
9. Ploetz M, Kirchebner B, Volk W et al. (2023) Influence of thermal process parameters on the properties of material jetted CuSn8 components. Materials Science and Engineering: A 871:144869. https://doi.org/10.1016/j.msea.2023.144869
10. Imani Moqadam S, Mädler L, Ellendt N (2019) A High Temperature Drop-On-Demand Droplet Generator for Metallic Melts. Micromachines 10:477. https://doi.org/10.3390/mi10070477

11. Arrizubieta JI, Ukar O, Ostolaza M et al. (2020) Study of the Environmental Implications of Using Metal Powder in Additive Manufacturing and Its Handling. Metals 10:261. https://doi.org/10.3390/met10020261
12. Kirchebner B, Rehekampff C, Tröndle M et al. (2021) Analysis of salts for use as support structure in metal material jetting. Prod Eng Res Devel 15:855–862. https://doi.org/10.1007/s11740-021-01055-1
13. Himmel B, Rumschoettel D, Volk W (2019) Tensile properties of aluminium 4047A built in droplet-based metal printing. RPJ 25:427–432. https://doi.org/10.1108/RPJ-02-2018-0039
14. Zhang D, Qi L, Luo J et al. (2017) Direct fabrication of unsupported inclined aluminum pillars based on uniform micro droplets deposition. International Journal of Machine Tools and Manufacture 116:18–24. https://doi.org/10.1016/j.ijmachtools.2017.01.001
15. Yi H, Luo J, Liu M et al. (2022) Metal droplet printing of tube with high-quality inner surface via helical printing trajectory and soluble support. Virtual and Physical Prototyping 17:582–598. https://doi.org/10.1080/17452759.2022.2058307
16. Zhou M, Liu Y, Wei C (2020) Topology optimization of easy-removal support structures for additive manufacturing. Struct Multidisc Optim 61:2423–2435. https://doi.org/10.1007/s00158-020-02607-2
17. Jiang J, Xu X, Stringer J (2018) Support Structures for Additive Manufacturing: A Review. JMMP 2:64. https://doi.org/10.3390/jmmp2040064
18. Ni F, Wang G, Zhao H (2017) Fabrication of water-soluble poly(vinyl alcohol)-based composites with improved thermal behavior for potential three-dimensional printing application. J Appl Polym Sci 134. https://doi.org/10.1002/app.44966
19. Hildreth OJ, Nassar AR, Chasse KR et al. (2016) Dissolvable Metal Supports for 3D Direct Metal Printing. 3D Printing and Additive Manufacturing 3:90–97. https://doi.org/10.1089/3dp.2016.0013
20. Lefky CS, Zucker B, Wright D et al. (2017) Dissolvable Supports in Powder Bed Fusion-Printed Stainless Steel. 3D Printing and Additive Manufacturing 4:3–11. https://doi.org/10.1089/3dp.2016.0043
21. Ozeryanaya IN (1985) Corrosion of metals by molten salts in heat-treatment processes. Met Sci Heat Treat 27:184–188. https://doi.org/10.1007/BF00699649
22. Nagaoka T, Kita K, Kondo N (2015) Hot corrosion of Al_2O_3 and SiC ceramics by KCl–NaCl molten salt. J Ceram Soc Japan 123:685–689. https://doi.org/10.2109/jcersj2.123.685
23. Kirchebner B, Ploetz M, Rehekampff C et al. (2021) Influence of Salt Support Structures on Material Jetted Aluminum Parts. Materials 14:4072. https://doi.org/10.3390/ma14154072
24. Li C-J, Li P, Wang K et al. (2014) Survey of Properties of Key Single and Mixture Halide Salts for Potential Application as High Temperature Heat Transfer Fluids for Concentrated Solar Thermal Power Systems. AIMS Energy 2:133–157. https://doi.org/10.3934/energy.2014.1.133
25. Wang Z, Wang H, Li X et al. (2015) Aluminum and silicon based phase change materials for high capacity thermal energy storage. Applied Thermal Engineering 89:204–208. https://doi.org/10.1016/j.applthermaleng.2015.05.037
26. Brandt R, Neuer G (2007) Electrical Resistivity and Thermal Conductivity of Pure Aluminum and Aluminum Alloys up to and above the Melting Temperature. Int J Thermophys 28:1429–1446. https://doi.org/10.1007/s10765-006-0144-0
27. Bale CW, Bélisle E, Chartrand P et al. (2016) FactSage thermochemical software and databases, 2010–2016. Calphad 54:35–53. https://doi.org/10.1016/j.calphad.2016.05.002